Journal of Power Sources 217 (2012) 417–430

Contents lists available at SciVerse ScienceDirect

Journal of Power Sources

journal homepage: www.elsevier.com/locate/jpowsour

Assessment of Alane as a hydrogen storage media for portable fuel cell power sources

Kyle N. Grew [a,*], Zachary B. Brownlee [b], Kailash C. Shukla [c], Deryn Chu [a]

[a] U.S. Army Research Laboratory, Sensors and Electron Devices Directorate, 2800 Powder Mill Road, RDRL-SED-C, Adelphi, MD 20783, USA
[b] U.S. Military Academy at West Point, Department of Civil & Mechanical Engineering, West Point, NY 10996, USA
[c] U.S. Army Natick Soldier Systems Center, 15 Kansas Street, Natick, MA 01760, USA

GRAPHICAL ABSTRACT

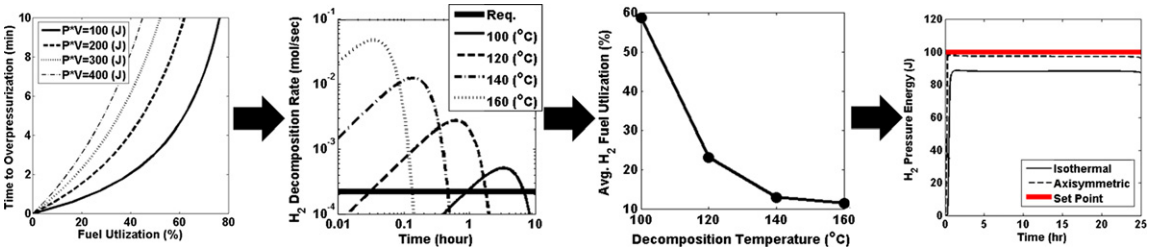

HIGHLIGHTS

- Alane (AlH_3) is examined as a H_2 source for portable power applications.
- A fuel cell-battery hybrid design considered.
- System analysis shows feasibility of device.
- Safety concerns regarding adequately controlling H_2 pressure.
- Thermal latency of thermal decomposition promotes need for onboard H_2 storage.

ARTICLE INFO

Article history:
Received 2 April 2012
Received in revised form
30 May 2012
Accepted 1 June 2012
Available online 13 June 2012

Keywords:
Portable
Alane
Hydrogen storage
Fuel cell

ABSTRACT

Aluminum hydride (AlH_3), often referred to as Alane, is examined as a hydrogen storage media for fuel cell-based portable power applications. The hydrogen storage capacity and thermally activated dehydrogenation of Alane makes it a candidate as a hydrogen storage material for portable fuel cell systems. In this study, Alane is found to provide a high gravimetric and volumetric energy density for portable power applications; however, there are significant challenges that must be addressed. These challenges include proper thermal control of the Alane dehydrogenation, fuel utilization and storage/treatment of excess hydrogen, and most importantly safety measures to prevent failure from an over-pressurization caused by excess hydrogen.

1. Introduction

The development of a safe and portable power source with high gravimetric and volumetric energy densities is a challenge of ongoing importance. For military and soldier-born applications, the U.S. Department of Defense *Operational Energy Strategy* report cites

* Corresponding author. Tel.: +1 301 394 3561; fax: +1 301 394 0273.
E-mail address: kyle.n.grew.ctr@mail.mil (K.N. Grew).

0378-7753/$ – see front matter © 2012 Elsevier B.V. All rights reserved.
http://dx.doi.org/10.1016/j.jpowsour.2012.06.007

reducing fuel demands, expanding energy storage and conversion options, and improving energy security as being critical to national security [1]. One of the report's findings is that there is a significant need to lighten the load (reduce mass) that our soldiers are required to carry. It estimates that in 2012, soldiers on three-day foot patrols in Afghanistan will each carry more than 50 batteries, with a mass of more than 8 kg (approx. 18 lbs) [1]. Energy storage and power requirements can be expected to increase with advances in electronics, sensors and communications equipment.

These details highlight the importance of energy storage and conversion technologies, and advocate sustained research and development efforts. Fuel cell systems are among the technologies being developed to help reduce the mass of present power sources. In principle, fuel cells offer several advantages over more traditional energy storage technologies. These benefits are derived from the large specific energies offered by the chemical energy stored in a host of fuels. This concept is shown in Fig. 1, which is a conceptual adaptation of a figure from Bostic et al. [2]. The fuel cell system has some baseline mass, which is offset by the large specific energy (i.e., gravimetric energy density) of the fuel. As the mission length and energy requirement increases, the specific energy of the fuel can result in a net mass savings relative to other portable power sources (e.g., batteries). Because of the initial mass of the fuel cell system, this mass savings occurs after some period of time.

Despite the substantial chemical energy stored in various fuels, it can be difficult to convert this energy into a usable (electrical) form. Complex fuels typically require additional balance of plant, which adds to the system's weight, size, and parasitic losses. For portable applications, simplicity is vital. Fuel selection for portable fuel cells requires that the fuel be adequate for use, safe to handle, storable, transportable, cost effective, and have large gravimetric and volumetric specific energies (i.e., high energy density). There are a range of choices, which are moderated as the fuel requirements are overlain with the needs for a small and lightweight system design. A liquid or solid fuel is ideal. For this reason many portable fuel cell systems use alcohol fuels, including numerous efforts with direct and reformed methanol [3,4], ethanol [3,4] and larger alcohols [3–5]. These fuels are stable in the liquid form, offering logistical advantages while providing large energy densities. Nitrogen bearing compounds (e.g., hydrazine hydrates) have also been reported [6–8], as have efforts with chemical- and metal-hydrides [9–11]. In this study, theory is used to examine Alane as a solid hydrogen storage material for use in a portable fuel cell system.

In practice Alane undergoes an endothermic dehydrogenation process as it is heated; Alane undergoes an endothermic dehydrogenation process; decomposing to Hydrogen (H_2) and Aluminum (Al). Alane provides a reasonable volumetric hydrogen capacity at a density of ρ_{AlH3}(=1480 kg m^{-3}) with a gravimetric H_2 capacity of greater than 10%wt [12]; a larger volumetric hydrogen capacity than liquid H_2 [13]. These benefits are significant, but using Alane also presents challenges.

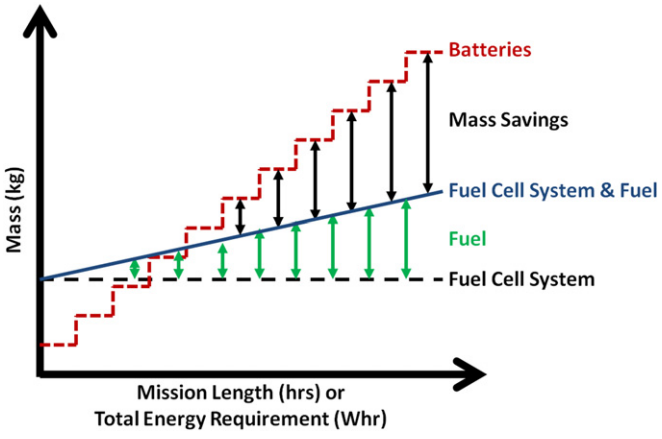

Fig. 1. The mass of energy storage and conversion materials is plotted as a function of mission length, or mission energy requirement.

Alane has a large hydrogen fugacity, prohibiting thermodynamic stability at room temperature. Only metastable polymorphic phases of Alane can be formed for applications near ambient conditions [14]. Metastable Alane can undergo a controlled thermal dehydrogenation under normal operating conditions. Noting that Alane has also been used in applications including inorganic explosives, reducing agents and solid rocket propellants, there are still inherent risks if it should be sufficiently perturbed [12]. Because of the hydrogen fugacity, Alane formation from the Al and H_2 constituents is not possible without extreme pressures. There have been recent efforts to improve processing methods [12]. For example, Graetz, Reilly and colleagues examined the use of Ti-doped Al powder and different amines to reversibly form AlH_3-amine adducts under modest H_2 pressures [14–21].

Probably the most significant challenge to the use of Alane in a portable fuel cell system is the safety risk associated with an over-pressurization. This refers to a condition where the H_2 pressure generated from the dehydrogenation process exceeds the pressures that the system can handle; either in a storage vessel or as it is fed to the fuel cell. Such a scenario could occur as a result of insufficient fuel utilization during operation, or if the Alane fuel was stored at a sufficiently elevated temperature. For portable fuel cell systems, the fuel side is often sealed with pressure relief. There is a need to intermittently purge contaminants and gases that can build up in the anode. To both safely operate and maximize the system's energy density, excess H_2 should not be purged on a regular basis. This presents a challenge because H_2 has a large specific volume of 11.9 m^3 kg^{-1} at ambient conditions. If it is not properly controlled and/or a runaway condition is encountered, the H_2 pressure can cause a catastrophic failure.

With these concerns, theory is developed and applied to explore Alane as a H_2 storage material for a portable, low temperature fuel cell system. This study will use a DuPont Nafion® based low temperature proton exchange membrane fuel cell (PEMFC); however, the results should also be suited to other types of low temperature fuel cell systems. The fuel cell system is hybridized with a battery, which is considered as a component of the system's internal balance of plant. For the purposes of this work, a conceptual system producing 30 W of continuous power is examined. This power is selected by assuming that roughly 20–25 W of continuous electrical power, with an additional 5–10 W of power being a conservative estimate of the requirements for the balance of plant. The fuel cell operates at 0.7 V/cell, standard for a Nafion based H_2/air PEMFC. The balance of plant requires fans to maintain proper air stoichiometry, sensors and logic controllers, power conditioning, a heater to support the thermal dehydrogenation of Alane, and recharging of the hybrid battery.

The remainder of the manuscript examines different aspects of operation, building to the calculated performance of such a portable fuel cell system. It is organized such that in section 2, the fuel utilization requirements for a fuel cell of arbitrary size to avoid over-pressurization are calculated, which serve as limits for the system development. Section 3 explores theory methods related to the thermal decomposition, or dehydrogenation, of the Alane. Details related to the extension of this decomposition process into the theoretical analysis of a conceptual fuel cell system are also examined in this section. This development includes theory related to heat transfer within the system, control system analysis, hydrogen storage, and identification of the relevant system and

material properties. Section 4 provides discussion relevant to the trends associated with the dehydrogenation of Alane and its implementation into the fuel cell system. Finally, concluding remarks are provided in section 5.

2. System requirements

Prior to exploring the thermal dehydrogenation of Alane, the requirements for the fuel cell system should be better qualified. Sizing calculations can be used understand how the system operation can have an effect on the possibility of an over-pressurization. This requires the fuel utilization η_{FU}, which is the ratio of the molar rates H_2 consumption $\dot{n}_{H_2}^{req.}$ to that dehydrogenated from the Alane $\dot{n}_{H_2}^{prod.}$.

$$\eta_{FU} = \frac{\dot{n}_{H_2}^{req.}}{\dot{n}_{H_2}^{prod.}} \quad \text{where} \quad \dot{n}_{H_2}^{req.} = \frac{I}{2F} = \frac{P_e}{2FV_e} \tag{1}$$

Faraday's law provides the rate at which the H_2 is consumed, using the current I, Faraday's constant F, the fuel cell's total electrical power P_e, and single cell operational voltage V_e. The molar rate of Alane's H_2 dehydrogenation, and that required by the fuel cell, can vary with time. Therefore, the moles of excess H_2, $n_{H_2}^{ex.}$, is calculated by integrating with respect to time t. This can be done discretely or approximated using the average fuel utilization $\overline{\eta_{FU}}$.

$$\begin{aligned} n_{H_2}^{ex.} &= \int_0^t \left(\dot{n}_{H_2}^{prod.} - \dot{n}_{H_2}^{req.}\right) dt \\ &= \int_0^t \dot{n}_{H_2}^{req.} \left(\frac{1}{\eta_{FU}(t)} - 1\right) dt \cong \frac{P_e}{2FV_e}\left(\frac{1}{\overline{\eta_{FU}}} - 1\right) t \end{aligned} \tag{2}$$

If the excess H_2 is stored in a pressure vessel, the ideal gas law to calculate the H_2 pressure. The H_2 pressure P_{H_2} is the total pressure in the pressure vessel of volume V_{ves}, at absolute temperature T_{ves} with the usual universal gas constant R.

$$P_{H_2} = n_{H_2}^{ex.} \frac{RT_{ves}}{V_{ves}} \tag{3}$$

Combining Eqs. (1)–(3) and simplifying, the average fuel utilization can be found.

$$\overline{\eta_{FU}^{req.}} = \frac{P_e RT_{ves} t}{P_e RT_{ves} t + 2FV_e P_{H_2} V_{ves}} \tag{4}$$

Eq. (4) allows the operational requirements to be input with those related to the H_2 pressure vessel. The fuel cell's fuel utilization can be input with the pressure vessel's maximum allowable pressure and volume to calculate the operational time until an over-pressurization condition occurs. The product of the maximum allowable volume and pressure of the pressure vessel are lumped as a single term maintaining units of work. This work is the energy associated with the pressurized volume. Its magnitude will influence the size, weight, and cost of the vessel.

In Fig. 2, the time to over-pressurization for a 30 W fuel cell operating at 0.7 V/cell is provided as a function of fuel utilization. Fig. 2(a) and (b) shows the fuel utilizations required at short (minutes) and long (hours) time-scales, respectively. These results assume the H_2 in the pressure vessel is at 80 °C, roughly between the fuel cell operation and Alane dehydrogenation temperatures. The pressure–volume terms are estimates of reasonable pressure and volume magnitudes, ranging from 100 J (approximately 0.2 L at 5 atm) to 400 J (approximately 0.4 L at 10 atm). The pressure–volume energy values were selected provide a reasonable volume for excess H_2 storage that should not be prohibitively expensive or heavy.

Fig. 2 reinforces concerns of over-pressurization. Fig. 2(a) suggests that if the fuel utilization should unexpectedly dip, an over-pressurization could occur in a matter of seconds to minutes. Such a scenario could arise from a change in power demands, extreme operational environments, Alane's dehydrogenation conditions, or fuel cell operational behavior. Over-pressurization concerns are not limited to event-driven unexpectedly low fuel utilization. There are also concerns at the longer time scales shown in Fig. 2(b). High fuel utilizations are required to operate for extended periods of time, requiring a great degree of control. Redundant safety measures will be needed to safely use Alane for a portable fuel cell system.

3. Methods: thermal dehydrogenation of Alane

3.1. Dehydrogenation properties and parameters

Noting the high fuel utilizations needed to avoid over-pressurization, it is necessary to understand the details of Alane's thermal dehydrogenation process. Graetz and Reilly have examined isothermal dehydrogenation of the α-, β-, and γ- polymorphs using

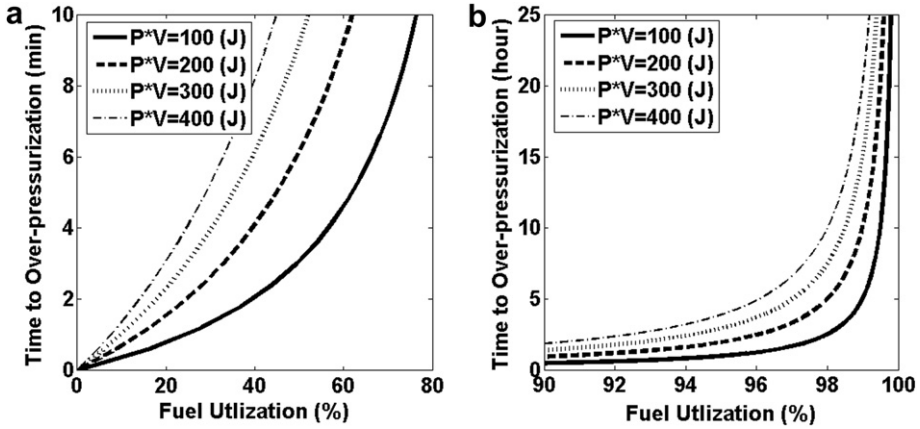

Fig. 2. The time until an over-pressurization condition is plotted as a function of fuel utilization, where trends represent a range of pressure-volume energy (work) limits for the internal storage of the H_2 gas. Results are provided for regions of (a) low and (b) high fuel utilization assuming the H_2 is at 80 °C and the fuel cell is producing 30 W of electrical power at 0.7 V/cell.

Table 1
Polymorph specific dehydrogenation properties of Alane.

Polymorph phase	Property	Value	Units	Reference
α	A_o	1.2×10^{10}	s^{-1}	[13]
β		8.8×10^{8}	s^{-1}	[13]
γ		8.5×10^{6}	s^{-1}	[13]
α	E_A	102.2	kJ mol^{-1}	[13]
β		92.3	kJ mol^{-1}	[13]
γ		79.3	kJ mol^{-1}	[13]
α	ΔH_R: α-$AlH_3 \rightarrow Al + 3/2H_2$	6.6 ± 0.4	kJ $mol_{H_2}^{-1}$	[25,26]
β	ΔH_{Trans}: β-$AlH_3 \rightarrow$ α-AlH_3	-1.0 ± 0.3	kJ $mol_{H_2}^{-1}$	[25,26]
γ	ΔH_{Trans}: γ-$AlH_3 \rightarrow$ α-AlH_3	-1.9 ± 0.3	kJ $mol_{H_2}^{-1}$	[25,26]

a reactor chamber, arriving at an exponential rate equation for the dehydrogenation process [13].

$$\alpha = 1 - \exp\left\{-(At)^b\right\} \quad \text{where } A = A_o \exp\left\{-\frac{E_A}{RT(t)}\right\} \tag{5}$$

Eq. (5) provides the extent of the dehydrogenation α as a function of time (and implicitly, temperature). The power $b(=2)$ indicates the type of growth during dehydrogenation, which is indicative of two-dimensional growth [13]. An Arrhenius rate constants A and activation energy E_A were fit for each of the polymorphs with an initial rate A_o. The values calculated by Graetz and Reilly are provided in Table 1 [13], which are used throughout this work.

The implementation of these rate expressions is shown in Fig. 3. The measured rate constants are compared to those calculated using Arrhenius forms in Fig. 3(a). Likewise, a measure of the isothermal dehydrogenation of the α-, β-, and γ- polymorphs at different dehydrogenation temperatures are provided as a function of time in Fig. 3(b)–(d). The symbols are the experimental data, which has been taken from Graetz and Reilly [13]. The model (lines) demonstrates that the dehydrogenation process has been accurately represented. The discrepancies between the experimental data and analytic expressions at the lower temperatures fall within the reported errors in the activation energies.

The dehydrogenation rate $d\alpha/dt$ is an equally important property. The time and temperature are implicitly linked in Eq. (5) (i.e., thermal history) so the rate change in temperature dT/dt also influences the dehydrogenation process. It is calculated using the chain rule.

$$\frac{d\alpha}{dt} = \frac{d\alpha}{dT}\frac{dT}{dt} = \exp\left\{-(At)^b\right\} b[At]^{(b-1)} A\left[\frac{tE_A}{RT^2}\frac{dT}{dt} + 1\right] \tag{6}$$

In Eq. (6), the rate of dehydrogenation is a function of the rate change in temperature, temperature, and time. The dehydrogenation rate is used extensively in this study as it is directly proportional to the molar H_2 decomposition rate.

3.2. Alane thermal dehydrogenation and hydrogen storage chamber

With rate expressions for the dehydrogenation process in place, a conceptual dehydrogenation and H_2 storage chamber can be examined. As will be shown in Section 3.7, the H_2 storage chamber is needed because of latency involved in the heating and cooling of the Alane during dehydrogenation. A system like

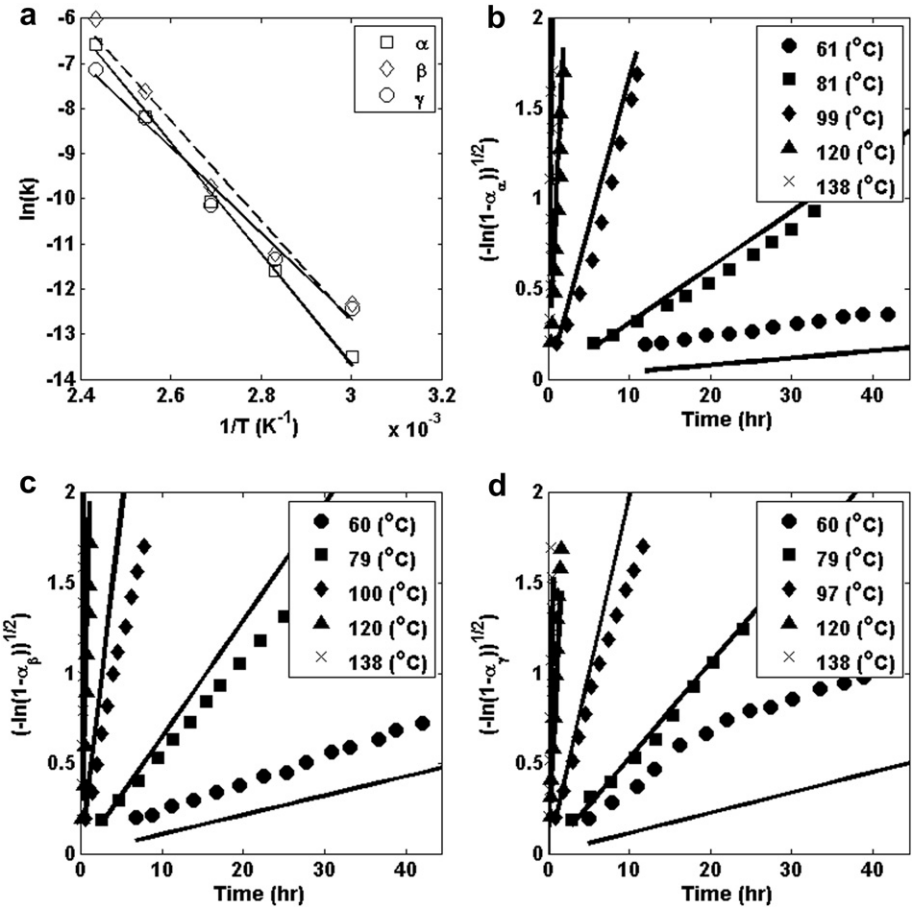

Fig. 3. Isothermal Alane dehydrogenation kinetics validation. The (a) Arrhenius rate constants and the isothermal dehydrogenation of the (b) α-, (c), β-, and (d) γ-Alane polymorphs are shown. Symbols are experimental data from Graetz and Reilly [13], and lines are the analytic results.

the schematic in Fig. 4 is considered. The Alane is taken as an annulus, secured onto a cartridge heater that is fixed on top of a cap. The cap can be married to an insulated re-sealable pressure vessel, enabling exhausted Alane to be replaced. It could be factory sealed to simplify the approach and improve safety; however, the entire vessel would need to be replaced as more fuel is needed, decreasing the system's energy density. This vessel serves both as the dehydrogenation chamber and H_2 storage container.

The H_2 storage chamber must incorporate a pressure regulator which dictates the pressure of the H_2 passed to the fuel cell, minimizing pressure gradients across the polymer electrolyte. A pressure transducer can be used to provide feedback to the cartridge heater. Pressure reliefs should also be incorporated so that excess H_2 pressure can be expelled prior to failure. This design is an oversimplification of an actual working system. Further engineering verification would be needed before integrating into an actual test system.

3.3. Isothermal dehydrogenation of Alane

Thermal dehydrogenation of the Alane can be examined using the energy equation.

$$\rho C_p\left(\frac{\partial T}{\partial t}+\vec{v}\cdot\nabla T\right) = \nabla(k\nabla T)+\frac{1}{V}\sum \dot{E}_i \tag{7}$$

Alane is a fixed solid mass, so the convective component of Eq. (7), $\vec{v}\cdot\nabla T$ is neglected. If isothermal conditions are assumed, Eq. (7) simplifies to a balance between the stored thermal energy and that of the sources and sinks.

$$\rho V C^p\frac{\partial T}{\partial t} = \dot{E}_S+\dot{E}_L+\dot{E}_R \tag{8}$$

The thermal energy stored in the Alane of density ρ, volume V, and specific heat C^p is proportional to source terms $\dot{E}_i$. The mass of the Alane m may be used in place of ρV.

Eq. (8) uses three source terms; beginning with the rate at which heat is supplied from heater $\dot{E}_S$ that drives the thermal dehydrogenation process. This heat source is dynamically controlled to maintain the appropriate thermal conditions. It is equal to the power provided to the Alane via the cartridge heater.

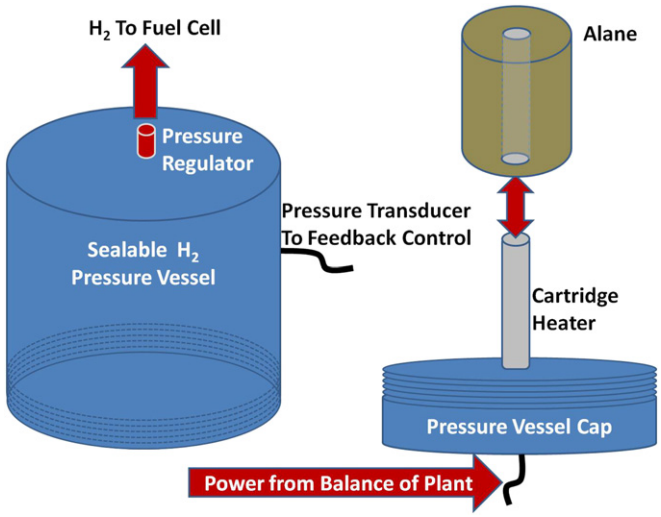

Fig. 4. A schematic of a thermal dehydrogenation and H_2 containment vessel.

The convection of heat to the surroundings occurs at an effective rate of $\dot{E}_L = R_{insu}^{eff^{-1}}[T-T_\infty]$. This loss is proportional to an effective insulation resistance R_{insu}^{eff} and ambient temperature T_∞. The effective thermal resistance is discussed in Section 3.7. The endothermic heat of reaction consumes heat at a rate $\dot{E}_R = m\gamma_o\Delta H_R(d\alpha/dT)(dT/dt)$, which is a function of the heat of reaction ΔH_R and the rate of thermal dehydrogenation of the Alane, $m\gamma_o(d\alpha/dT)(dT/dt)$. Plugging these terms into Eq. (8), the rate change in the temperature is derived.

$$\frac{dT}{dt} = \frac{\left[\dot{E}_S-\frac{(T-T_\infty)}{R_{ins}}-m\gamma_o\Delta H_R bA^b t^{b-1}\exp\left\{-(At)^b\right\}\right]}{\left[mC_pRT^2+m\gamma_o\Delta H_R E_a b(At)^b\exp\left\{-(At)^b\right\}\right]}RT^2 \tag{9}$$

Eq. (9) is a non-linear, ordinary differential equation (ODE), subject to the initial condition of the initial temperature of the Alane T_o. The extent and rate of dehydrogenation from the Alane are calculated with Eqs. (5) and (6) once the temperature-time dependencies are known.

3.4. Axisymmetric model of the dehydrogenation of Alane

Returning to Eq. (7), the energy equation can be expanded for the non-isothermal system. Alane's modest thermal conductivity can promote non-uniform temperatures. Assuming the Alane is an axisymmetric annulus, Eq. (7) can be expanded in the radial direction,

$$\rho C^p\frac{\partial T}{\partial t} = \frac{1}{r}\frac{\partial}{\partial r}\left(rk\frac{\partial T}{\partial r}\right)+\rho\gamma_o\Delta H_R\frac{d\alpha}{dt} \tag{10a}$$

subject to the initial and boundary conditions.

$$T = T_o \quad t = 0,\ r \tag{10b}$$

$$q''\cdot A = \dot{E}_S \quad t, r = R_{id} \tag{10c}$$

$$q''\cdot A = \frac{(T-T_\infty)}{R_{insu}^{eff}} \quad t, r = R_{od} \tag{10d}$$

In Eq. (10a), $d\alpha/dt$ is equal to the analytic expression, Eq. (6). The boundary conditions in Eqs. (10c) and (10d) prescribe the heat flux q'', from the heater and convection processes respectively. Solving Eq. (10), provides the spatial and temporal distributions of the temperature within the Alane. This enables the extent and rate of dehydrogenation can be calculated locally within the Alane with Eqs. (5) and (6).

3.5. Control of the hydrogen dehydrogenation and storage processes

Heat supplied by the cartridge heater requires feedback control. The rate change in the dehydrogenation $d\alpha/dt$ in Eq. (9) or (10), can be used to with the molar ratio $\gamma_o(=0.05(\text{mol } H_2/g_{AlH_3}))$ identify the molar rate of H_2 being released from the Alane $\dot{n}_{H_2}^{prod.}$.

$$\dot{n}_{H_2}^{prod.} = m\gamma_o\frac{d\alpha}{dt} = m\gamma_o\frac{d\alpha}{dT}\frac{dT}{dt} \tag{11}$$

Implementing the ideal gas law, the difference between the molar rates of H_2 produced from the Alane and that which was consumed by the fuel cell can be integrated to calculate the energy attributed to the pressure–volume term.

$$PV_{H_2}^{res} = RT_{res}\int_0^t \left(\dot{n}_{H_2}^{prod.} - \dot{n}_{H_2}^{req.}\right)dt$$
$$= RT_{res}\int_0^t \left(m\gamma_o \frac{d\alpha}{dT}\frac{dT}{dt} - \frac{P_e}{2FV_e}\right)dt \quad (12)$$

The pressure–volume energy in the reservoir $PV_{H_2}^{res}$ is a cumulative function of time. It can increase or decrease depending upon the rates of H_2 production and consumption. This property is easily measured, making it ideal for feedback control. It is used to provide the appropriate power the heater during dehydrogenation. For simplicity, a proportional control is considered.

$$\dot{E}_S = \begin{Bmatrix} Q_s^{max} & PV(t) \le PV_{min} \\ K_p\left[\frac{PV_{S.P.} - PV(t)}{PV_{S.P.}}\right]Q_s^{max} & PV_{min} < PV(t) < PV_{S.P.} \\ 0 & PV(t) \ge PV_{S.P.} \end{Bmatrix} \quad (13)$$

In Eq. (13), the rate at which energy is delivered by the heater $\dot{E}_S$ to the Alane is set by the difference between the pressure–volume energy in the H_2 reservoir $PV(t)$ and the set point $PV_{S.P.}$. If below a critical threshold PV_{min}, the heater is set to deliver the maximum power Q_s^{max}. This threshold is that which is needed to provide H_2 to the fuel cell at 1 atm total pressure. While discussed in further detail in section 3.7, PV_{min} and $PV_{S.P.}$ are set to 35 J and 100 J, respectively, in this study. Once there is sufficient H_2 pressure to operate the fuel cell a proportional constant K_p, taken as unity here, scales the product of the maximum power that the heater can provide Q_s^{max} and the relative error. If the pressure–volume energy exceeds that of the set point, no power is provided to the heater. More robust control schemes are possible, but not considered at this time.

3.6. Solution procedures

Eqs. (9) and (11)–(13) describe the thermal dehydrogenation of Alane for a fuel cell. It serves as the baseline for this study. Because of the non-linear form of the equation, analytic solutions are not easily obtained. A 4'th order Runge–Kutta ODE solver with a fixed step size is used in this study. A fixed step size is used so that discreet sampling frequency of the heat source controller can be mimicked. The heat source is updated on a predefined frequency. The calculations are repeated with a range of step sizes to ensure the results are not a spurious result of the step size. This model provides the flexibility to explore sizing and pertinent limits of the system, as well as verification of the more complex non-isothermal model. Implementation of the scheme has been verified by comparing results to adaptive step ODE solvers, adjusting the grid density, and adjusting the frequency of the feedback controller. The axisymmetric system described in Eqs. (10)–(13) is a non-linear parabolic partial differential equation (PDE). A custom-written axisymmetric finite volume method (FVM) is used to solve the corresponding physics. This FVM method accounts for the nonlinearities introduced by the source term in Eq. (10). It is a semi-implicit FVM formulation, which resembles a fully implicit scheme. Temperature values from the previous time step being used in the non-linear terms introduced by the Alane dehydrogenation process. The temporal and spatial grid density has been examined to ensure that stable, grid independent solutions. Grid independence was identified at approximately 1×10^4 time steps over a 25 h period (9 s steps). The results provided in this study consider 2×10^4 time steps. Grid independence was recognized around 100–200 finite volumes, with 301 finite volumes being used for the results provided.

3.7. Properties related to sizing of Alane, pressure vessel, heater, and hybrid battery

Additional calculations are necessary to evaluate a practical fuel cell system using Alane. This begins with the mass of the Alane cartridge that is to be used. The capacity for the ideal two-electron electrochemical H_2 oxidation is $C_{H_2}^{ideal} = 2F/MW_{H_2} (= 26.8\ \text{A h g}_{H_2}^{-1})$. The H_2 occupies 10 %wt of the Alane mass, meaning the mass of the H_2 contained in the Alane is $m_{H_2} = 0.10 m_{Al\ H_3}$. Assuming all of the H_2 can be decomposed, the mass of Alane needed to operate the fuel cell for a specified period of time can be determined.

$$m_{AlH_3} = \frac{P_e \cdot t}{0.1 \cdot C_{H_2}^{ideal} \cdot V_e \cdot \eta_{FU}} \quad (14)$$

At 100% fuel utilization, approximately 16 g of Alane are required per hour of operation for a fuel cell producing 30 W of power at 0.7 V/cell. Therefore, 0.4 kg of Alane can provide up to 25 h of operation while occupying a volume of 0.27 L. This is used as a baseline.

As the Alane decomposes, its properties change. Chemical and metal hydrides are known to have significantly different thermal conductivities than their individual chemical constituents. Therefore, the thermal conductivity is prescribed using a linear dependence on α, $k = (1-\alpha)\cdot k_{AlH_3} + \alpha \cdot k_{Al}$. The mass, density, and specific heat are assumed to follow an analogous functional form. Alane's thermal conductivity $k_{AlH_3} (= 0.5\ \text{W}\cdot\text{m}^{-1}\cdot\text{K}^{-1})$, density $\rho_{AlH_3} (= 1480\ \text{kg}\cdot\text{m}^{-3})$ [13], and specific heat $C_{AlH_3}^p (= 1333\ \text{J}\cdot\text{kg}^{-1}\cdot\text{K}^{-1})$ [22] are taken from the literature. The thermal conductivity is estimated for typical metal and chemical hydrides [23]. The corresponding property values for pure Aluminum are $k_{Al} (= 237\ \text{W}\cdot\text{m}^{-1}\cdot\text{K}^{-1})$, $\rho_{Al} (= 2700\ \text{kg}\cdot\text{m}^{-3})$, and $C_{Al}^p (= 903\ \text{J}\cdot\text{kg}^{-1}\cdot\text{K}^{-1})$ [24]. As depicted in Fig. 4, the Alane is taken to be an annulus with a cartridge heater at the core. The inner and outer radii of the Alane are R_i(=0.01 m) and R_o(=0.03 m), indicating an height of L_{an}(=0.108 m). To limit the size of the heater and hybrid battery, the heater is limited to a maximum output of 25 W.

In Section 3.2, it was suggested that the Alane dehydrogenation chamber should also be used to storage of excess H_2. This is a result of the latency introduced by thermal mass of the Alane. This latency can be shown more rigorously by demonstrating the heat rate and power requirements for control of the Alane. Eqs. (1) and (11) are equated to calculate the required rate change in temperature dT/dt as a function of T and α. The time corresponding to each T and α is calculated using Eq. (5). Eq. (8) is used to calculate the (heat) power that must be supplied and/or removed to accommodate this rate change in temperature. In calculating the power, the rate of dehydrogenation for the heat of reaction is approximated with Eq. (1). Convective losses are neglected here. Fig. 5(a) provides the heat rate required for a 30 W fuel cell operating at 0.7 V/cell on 0.4 kg of Alane. The power that must be added (positive) or removed (negative) from the Alane is provided in Fig. 5(b). To complement the 30 W fuel cell system, conditions related to 0 W are equally as important. The thermal energy of the Alane must be dissipated during shut down to avoid over-pressurization. These results are provided for the heat rate in Fig. 5(c) and the (heat) power in Fig. 5(d).

Several facets of Alane's dehydrogenation can be observed. In Fig. 5(a) and (b), the Alane must be slightly cooled to maintain a constant dehydrogenation rate. This means that only part of the endothermic heat of reaction must be recovered to maintain a constant dehydrogenation rate, reducing the overall heat that must be provided by the cartridge heater. If the Alane should reach temperatures above 100 °C, a second phenomenon is recognized. To maintain the necessary dehydrogenation rate, the Alane must be cooled faster than the endothermic heat of reaction (approximately

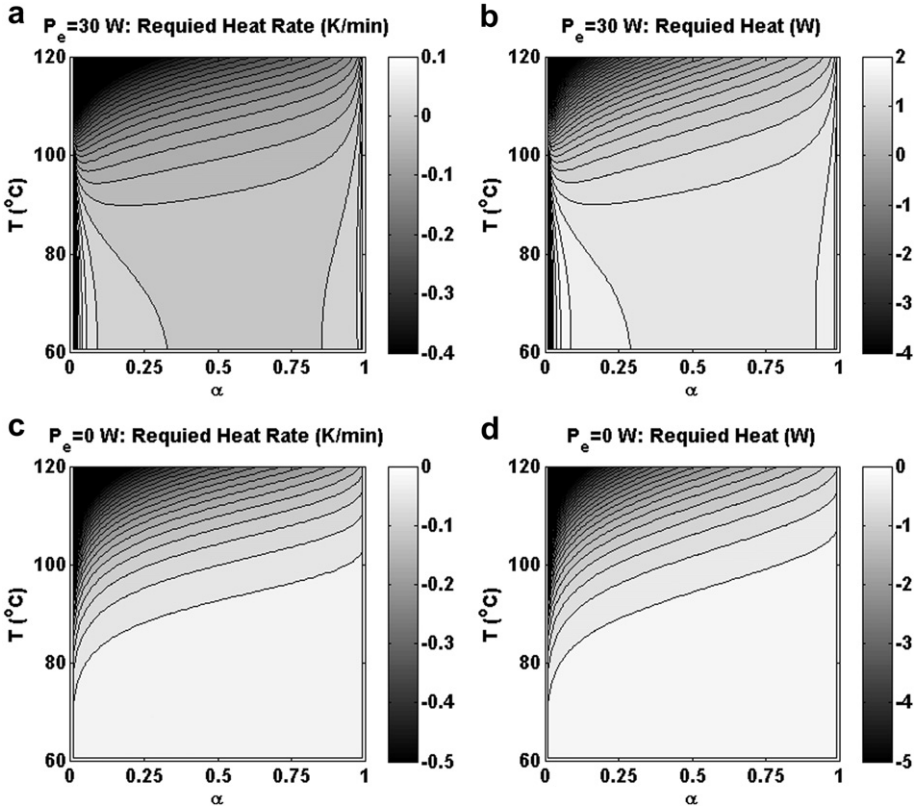

Fig. 5. The (a) heat rate and (b) heat needed to maintain the dehydrogenation of 0.4 kg of Alane during operation for a 30 W fuel cell system at 0.7 V/cell. The (c) heat rate and (d) heat needed to heat/cool the Alane as the fuel cell is shut off to 0 W is also provided.

1.5 W at 30 W and 0.7 V/cell) allows. This occurs with no heat being provided by the cartridge heater and indicates H_2 pressure will build for a period of time. Similar issues are observed in Fig. 5(c) and (d), when the dehydrogenation process needs to be stopped. Significant cooling rates, which can exceed those of the heat of reaction, are needed to quench the dehydrogenation process. When designing a control system, the limits of the controllers (the cartridge heater and heat of reaction) should exceed those that can be needed based upon the limits of the operational domain. Here, there are domains that have heating and cooling requirements exceeding the limits of the system. These domains will undoubtedly introduce latency into the response, during which H_2 pressure can build.

Because of potential issues with latency, the decomposition and storage unit discussed in Section 3.2 is incorporated in the remainder of the fuel cell system analyses. This vessel stores excess H_2, so there is sufficient H_2 available while also helping to protect the system from over-pressurizing. It is assumed that the pressure vessel has 0.3 L of free space and can maintain a maximum pressure of 8 atm (approximately 250 J). To avoid a pressure differential across the membrane electrolyte, the fuel cell should operate under about 1 atm pressure at the anode. The pressure vessel must first contain sufficient H_2 and so the system is set to run off of the hybrid battery until there are at least 35 J worth of H_2 pressure–volume energy available (approximately 1.15 atm). A set point of $PV_{S.P.}$(=100 J) is used, which provides sufficient H_2 pressure–volume energy to operate the fuel cell while also proving a factor of safety of 2.5 in terms of reaching the (assumed) critical pressure for the vessel. There is some flexibility in this selection; however, control becomes increasingly complex as it approaches 35 J.

The Alane dehydrogenation chamber and pressure vessel should also be insulated to minimize convective losses. At a total volume of V_{ves}(=0.6 L) (Alane, heater, and H_2 storage), we assume the chamber to by cylindrical with a height of L_{ves}(=0.127 m) and radius of R_{ves}(=0.039 m). This provides an effective external area of A_{ves}(=0.04 m^2). A t_{ins}(=0.01 m) Aerogel insulation can be used on the exterior, which has a thermal conductivity of k_{ins}(=0.013 W m^{-1} K^{-1}). This value is based on technical specifications of Thermablock, Inc. (Tampa, FL) Aerogel insulation materials. At 100 °C and 20 °C, the H_2 and air have a thermal conductivity of k_{H2}(=0.226 W m^{-1} K^{-1}) and k_{air}(=0.028 W m^{-1} K^{-1}) [24]. A non-dimensional analysis using a constant temperature Nusselt number $Nu = hL/k = 3.66$, provides convection coefficients of h_{H_2}(= 6.51 W·m^{-2}·K^{-1}) and h_{air}(=0.82 W m^{-2} K^{-1}). These can be used with the properties of the Aerogel to calculate an effective thermal resistance.

$$R_{ins}^{eff} = \sum R_i = \frac{1}{h_{H_2} A_{ext}} + \frac{t_{ins}}{k_{ins} A_{ext}} + \frac{1}{h_{air} A_{ext}} \quad (15)$$

The effective thermal resistance assumes that the H_2 takes on the mean temperature of the Alane. Using Eq. (15), an effective insulation resistance of R_{ins}^{eff}(= 53.7 K·W^{-1}) has been determined.

Because R_{ins}^{eff} is large, convective losses can be neglected while estimating the power P_s^{req} and energy E_s^{req} requirements for startup with the hybrid battery.

$$P_s^{req} = \rho V C^p \frac{dT}{dt} + \Delta H_R \cdot \frac{\dot{n}_{req}}{\eta_{F.U.}} \quad (16)$$

$$E_s^{req} = \int_{t_o}^{t_{start}} P_s^{req}\, dt \quad (17)$$

Eq. (16) has two components, the first is the power required to increase the temperature of the Alane from an initial temperature,

taken here as T_o(=20 °C), to the dehydrogenation temperature T_d, approximated as T_d(=100 °C). Rather than explicitly defining the heat consumed by the dehydrogenation process, it can be estimated using $\dot{n}_{req}$, which was defined in Eq. (1). The fuel utilization η_{FU} has also been included in Eq. (16); however, this should approach 100% because of the anode is sealed. Finally, the endothermic heat of reaction is provided in Table 1, where the α-polymorph is used. Eq. (17) provides the total energy required to startup the fuel cell. These equations can also be recast to include the 25 W of usable electrical power that the system is designed to provide the user during the startup by adding it to Eq. (16) and re-integrating Eq. (17). This would be characteristic of an instant power start.

Using Eqs. (16) and (17), approximations of the battery requirements are provided as a function of the startup time in Fig. 6. In Fig. 6, 25 W of power are required to heat the Alane from 20 °C to 100 °C over a 30 min startup period, requiring 12.6 W h of energy. If an additional 25 W of continuous power for the user in an instant-on mode are included, 25.1 W h of energy of energy is required. These values can be decreased by reducing the mass of the Alane in the cartridge. This allows a hybrid battery to be selected. A Yardney Technical Products, Inc. (Pawcatuck, CT) NCP7-3 Model LP31790 rechargeable Lithium ion battery is used as the basis for this study. This battery is specified with a 7.5 A h capacity at 3.6 V, with a volume of 0.104 L, and mass of 0.245 kg. This battery was selected because it can provide up to 25 W to a cartridge heater at a nominal discharge of approximately 1 C to prepare the fuel cell for operation. At approximately 2 C, the battery can provide an additional 25 W of electrical power to the user. Nominally, it has 27 W h of energy, meaning it has sufficient capacity to power the system under these conditions. The battery also enables the hybrid system to respond to demands for a peak continuous power of more than 150 W and 275 W for short durations (0.1 s pulse) once recharged by the fuel cell.

4. Discussion

The importance of maintaining high fuel utilizations was highlighted in qualifying the fuel cell system requirements in Fig. 2 (section 2). High fuel utilizations and corresponding control of the Alane's dehydrogenation process are needed to avoid over-pressurizing the H_2 storage tank. Prior to examining these issues with the integrated fuel cell system, the thermal dehydrogenation of Alane (by itself) is explored. The dehydrogenation is much more complex than what one may initially envision, meaning aspects including the specific polymorphs, dehydrogenation temperature, mass, heat rate, and thermal/dehydrogenation history of the Alane must be considered. Following the exploration of Alane's dehydrogenation process, it is extended to consider a portable fuel cell system.

4.1. Properties of the controlled dehydrogenation of Alane

Aspects including the effects of the specific Alane polymorphic phases, dehydrogenation temperature, initial mass, and heat rate on the characteristics of the dehydrogenation process are considered in this section. These characteristics are explored in Figs. 7–10, which make use of Eq. (11). To better understand these characteristics, isolated samples of Alane with no storage of the excess H_2 is considered. The results assume the fuel cell consumes H_2 at a constant molar rate, which supports a 30 W fuel cell at 0.7 V/cell. Fuel utilizations are calculated relative to the molar rate. Average fuel utilizations include only the periods that sufficient H_2 is being dehydrogenated from the Alane to power the fuel cell. Unless otherwise noted, the analysis will consider 0.2 kg of the α-polymorph at an isothermal decomposition of 100 °C.

Beginning with Fig. 7, the features attributed to the dehydrogenation of the α-, β-, and γ- polymorphic phases of Alane are considered. In Fig. 7(a), a log plot of the molar H_2 dehydrogenation rates are shown as a function of time. The dehydrogenation rates are compared to the molar rate of H_2 that would be required by an actual fuel cell, which appears as a constant horizontal line. The H_2 dehydrogenation has a rather non-uniform shape with some minor differences between the dehydrogenation rates of the respective polymorphs. The dome shape indicates that isothermal dehydrogenation of any polymorph will result in times where there is insufficient and excess H_2 being provided to the fuel cell, which can lead to periods of starvation and low fuel utilization if not properly accounted for. This shape is characteristic of the Alane dehydrogenation process and will be observed in the proceeding figures in this section. Because of concerns with low fuel utilization, which can lead to over-pressurization in an actual system, Eqs. (1) and (11) are also used in to provide the H_2 fuel utilization as a function of time in Fig. 7(b). The fuel utilization is averaged in Fig. 7(c), which does not incorporate periods that the H_2 dehydrogenation rate is insufficient to fuel the fuel cell. In Fig. 7(b), the fuel utilizations are quite low at the maximum dehydrogenation rates. In Fig. 7(c), the average fuel utilizations are recognized between 40% and 60%.

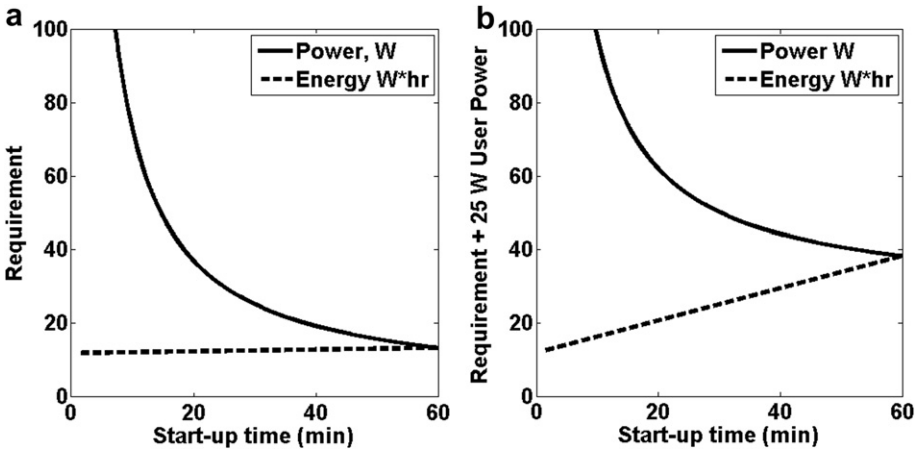

Fig. 6. The (a) power and energy requirements for the fuel cell startup is shown, and (b) requirements including an additional 25 W for the user in an instant-power scenario, which are used for hybrid battery sizing. Calculations assume ideal fuel utilization, dehydrogenation and ambient temperatures of 100 °C and 20 °C respectively, and a molar dehydrogenation rate equal to that which is required for the fuel cell.

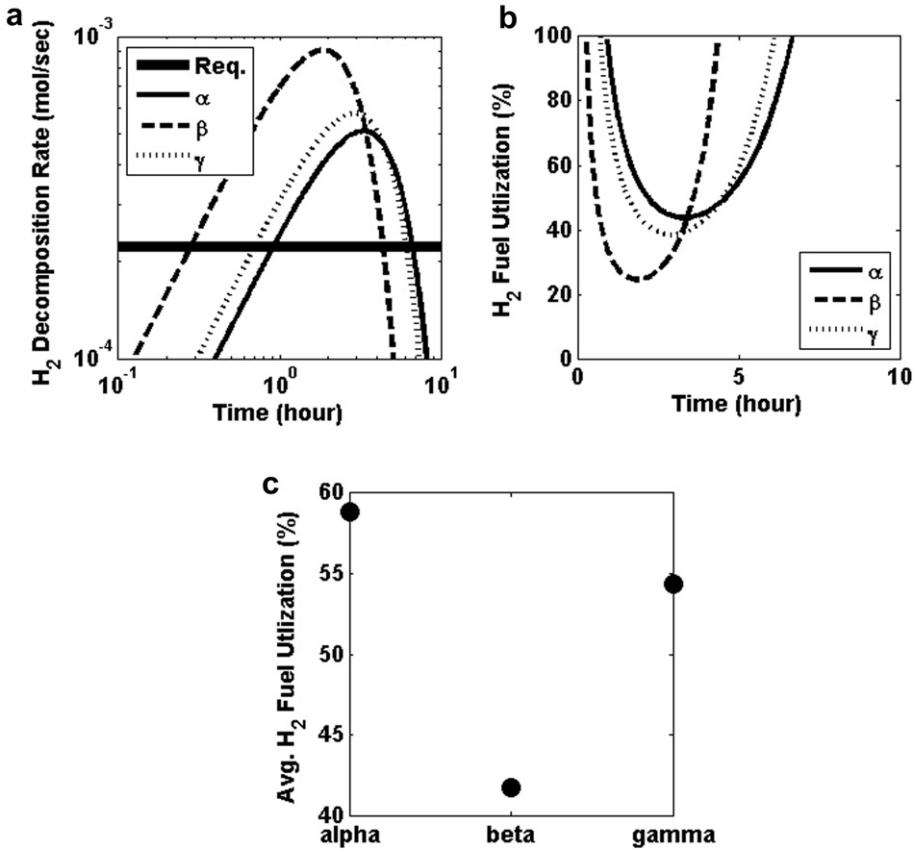

Fig. 7. Dehydrogenation of 0.2 kg of Alane at 100 °C is examined for the α-, β-, and γ-polymorphic phases. The (a) H_2 molar dehydrogenation rates, (b) percent H_2 fuel utilization are shown as a function of time, and (c) average percent H_2 fuel utilization are shown.

Moving to Fig. 8, the effect of the dehydrogenation temperature is examined. Fig. 8(a) provides a log plot of the molar H_2 dehydrogenation rate as a function of time. The H_2 fuel utilization is shown as a function of time in Fig. 8(b), with averages provided in Fig. 8(c). Higher dehydrogenation temperatures yield higher dehydrogenation rates and lower fuel utilizations. The dehydrogenation temperature also plays a significant role in terms of the time it takes the Alane dehydrogenation to reach that required by the fuel cell, as well as how long it will decompose.

Fig. 9 provides molar H_2 dehydrogenation rates and fuel utilizations different masses of Alane. The same dome shape of the molar H_2 dehydrogenation rate with respect to time that has previously been noted is also observed in Fig. 9(a). It is shown on a linear scale to better accentuate the scalar effects of the mass. The initial mass of Alane dictates the net H_2 and therefore total energy available. However, it also plays into the dehydrogenation temperature. For example, 50 g of Alane decomposing at 100 °C does not provide sufficient H_2 to power the fuel cell. However, if the dehydrogenation temperature were raised to 120 °C it would (not shown). This emphasizes the interplay between the choices in designing the system. The H_2 fuel utilization is provided as a function of time in Fig. 9(b) and the average fuel utilization are provided as a function of the initial Alane mass in Fig. 9(c).

Related to the dehydrogenation temperature and mass of Alane are the effects of the heating rate, taken here as the rate change in temperature. Examining Eq. (6), the rate change in dehydrogenation is a superposition between that resulting from the Alane temperature (i.e., dehydrogenation temperature above) and that at which it is being heated. To explore in inclusion of the rate change in temperature, Fig. 10 examines the H_2 dehydrogenation from the Alane at several rates of temperature increase. Because of the constant rate change in temperature, the temperature of the Alane is a linear function of time. An initial Alane temperature of 20 °C is used for all cases. The rate of H_2 dehydrogenation from the Alane is shown as a function of time in Fig. 10(a) for several heating rates. Likewise, the H_2 fuel utilization is shown as a function of time in Fig. 10(b). Because of the interplay between the time and temperature, these same trends are shown as a function of temperature in Fig. 10(c) and (d), respectively. The characteristic dome shape is again observed with respect to the molar H_2 dehydrogenation rate. It's location with respect to the time and temperature scales, as well as its magnitude, are functions of the rate change in temperature. The larger the rate change in temperature, the quicker the Alane reaches higher temperatures. This leads to larger dehydrogenation rates. On the other hand, those at lower rate change in temperature take longer to reach a temperature where H_2 dehydrogenation occurs at a reasonable rate and release the stored H_2 before they can reach the same temperatures. Larger H_2 dehydrogenation rates lead to greater risk of over-pressurization. As evident in Figs. 7–10, there is a direct need for hybridization with a battery to provide power and heat during times where there is insufficient H_2 dehydrogenation. Even under isothermal conditions, there is a period of time where the H_2 dehydrogenation rate is insufficient to power the fuel cell. This is evident in Figs. 7(a), 8(a) and 9(a). Even during heating the Alane in Fig. 10(a) and (b), there is a period of time until the dehydrogenation rate is sufficient to power the fuel cell. It may also be noted in Figs. 7–10 that dynamic control of the dehydrogenation process is needed to boost fuel utilization and avoid an over-pressurization. The risk of over-pressurization is highlighted by comparing the relatively low fuel utilizations recognized in

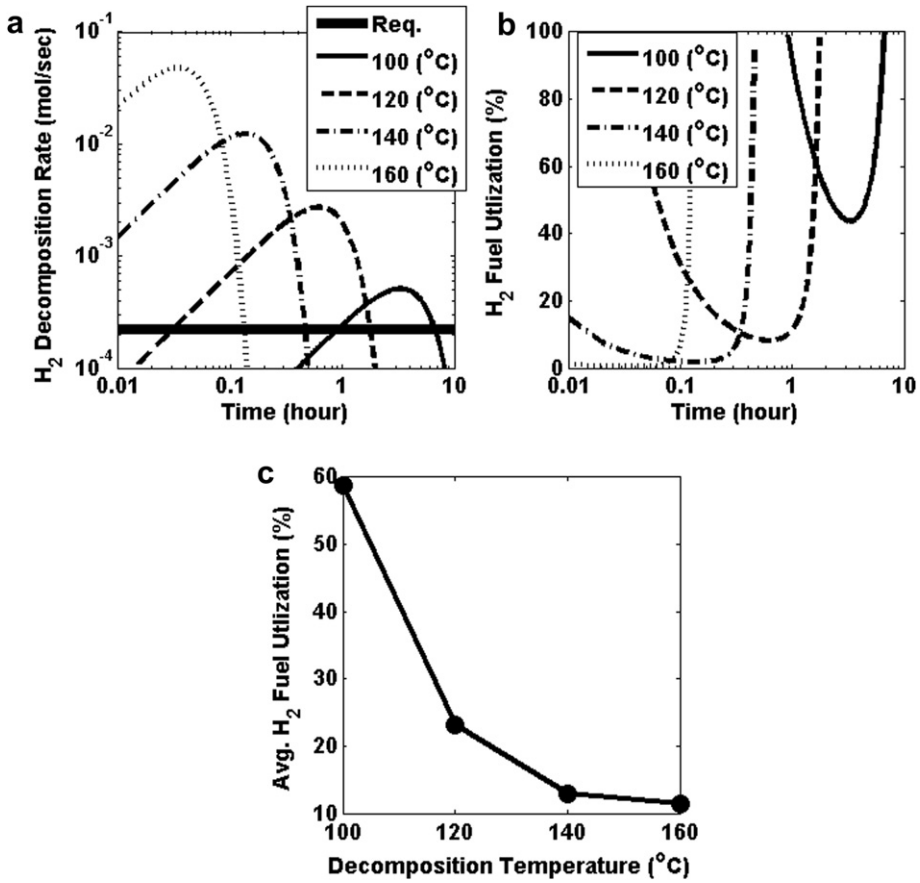

Fig. 8. Isothermal dehydrogenation of 0.2 kg of α-Alane is examined as a function of the dehydrogenation temperature. The (a) H_2 molar dehydrogenation rates and (b) percent H_2 fuel utilization as a function of time, and (c) average percent H_2 fuel utilization are shown.

Figs. 7–10 to the corresponding trends in Fig. 2. At these fuel utilizations, regardless of the H_2 storage unit considered, over-pressurization will occur in a matter of minutes. By moving to a controlled dehydrogenation process, these risks can be mitigated. This will improve fuel utilization and extend the time the fuel cell can operate at the required power (i.e., improve gravimetric energy density). However, an inability to properly control the dehydrogenation process will undoubtedly lead to an over-pressurization condition and risk of catastrophic failure. These considerations are undertaken in the subsequent section.

4.2. Analysis of Alane dehydrogenation for use in a portable fuel cell

With an understanding of the thermal dehydrogenation of Alane under controlled conditions, it is possible to examine its integration into the fuel cell system. First, a comparison between the isothermal and axisymmetric models is provided. Comparisons of the temperature and heat rates (i.e., rate change in temperature) for the respective models are provided in Fig. 11(a) and (b). The extent of the dehydrogenation process and the pressure–volume energy accumulated in the dehydrogenation chamber and H_2 storage vessel are also provided in Fig. 11(c) and (d). These results assume the fuel cell system operating at the previously described conditions, with an initial mass of 0.4 kg of α-Alane at room temperature in an evacuated dehydrogenation chamber.

For the axisymmetric model, a volume weighted mean temperature, heat rate, and extent of Alane dehydrogenation are provided in Figs. 11(a)–(c). Comparable trends are established with the two approaches. This verifies and provides confidence in the accuracy of the models. Radial temperature, heat rate, and degree of dehydrogenation distributions within the Alane are available, but are too small to discern at these time scales. However, there are minor discrepancies in the mean temperature, heat rate, and H_2 pressure–volume energy accumulated. Most pronounced are the variations during the initial heating of the Alane, which are the result of the variations in dehydrogenation properties attributed to the treatment of the Alane as a lumped isothermal system with volumetric source terms versus as axisymmetric with discrete boundary conditions. Because of these discrepancies, the axisymmetric model is used for the remainder of the work. Importantly, the H_2 pressure–volume energy stays below the set point and the 250 J critical rupture threshold for the system design under normal operation in Fig. 11(d). This does not take into account possible events like power requirement surges, changes in conditions, system shut down, or any disruptions or failures to the corresponding equipment.

As verification of the development of the framework, it can be noted that the Alane was able to power the system for approximately 25 h. This matches the calculations from Section 3.7, where it was noted that the system should operate for approximately 25 h on 0.4 kg of Alane. The slight uptick in temperature in Fig. 11(a) and decrease in the H_2 pressure–volume energy accumulated in Fig. 11(d) are the onset of the complete dehydrogenation of the Alane. Further validation is provided in Fig. 12, which provides the power and energy requirements for the system. In Fig. 12(a), it is seen that the heater provides 25 W of power until there is sufficient H_2 pressure in the chamber to power the fuel cell (i.e., 35 J). Once the H_2 pressure–volume energy reaches the minimum for the fuel

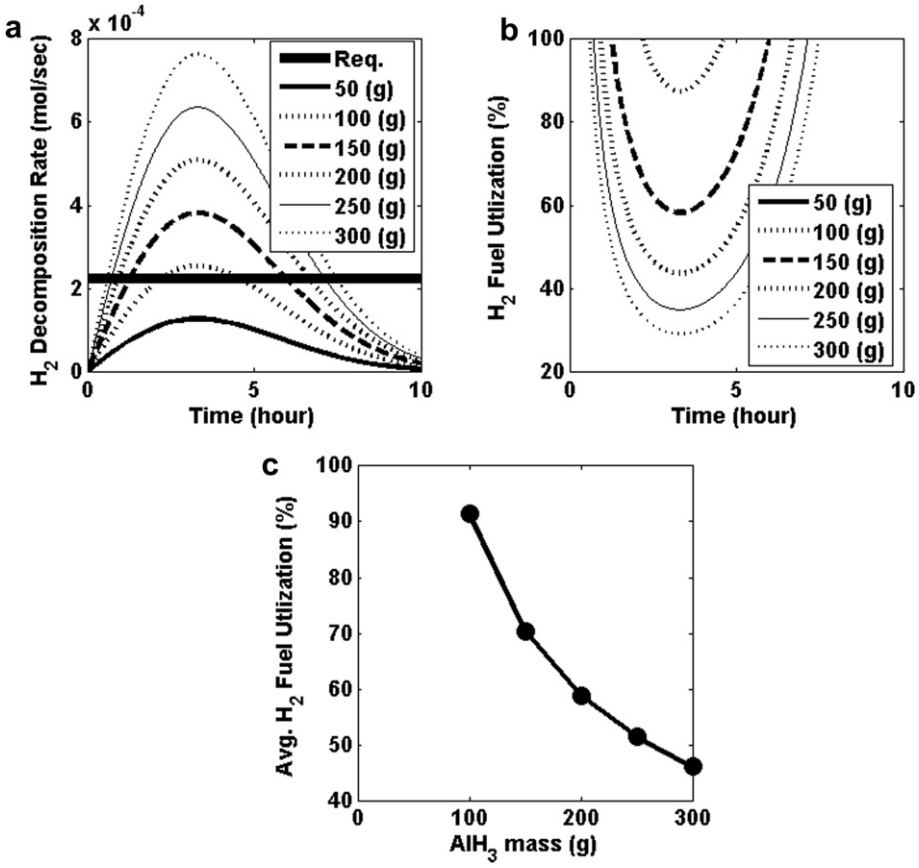

Fig. 9. Isothermal dehydrogenation of α-Alane at 100 °C is examined as a function of the mass of Alane. The (a) H_2 molar dehydrogenation rates, (b) percent H_2 fuel utilization as a function of time, and (c) the average percent H_2 fuel utilization are provided.

cell to operate, the Alane only needs to be heated to the extent that it sustains a dehydrogenation rate that is sufficient for maintaining the pressure–volume energy. The sustaining power required by the heater is roughly equivalent to the heat loss through the chamber and that of the endothermic heat of reaction. This loss is primarily attributed to the endothermic heat of reaction, which is calculated to be about 1.5 W. During the bulk of the operation the heater is providing 0.5–1 W of power to the Alane. The difference between that which is calculated and observed in the model is the result of the non-linear Alane dehydrogenation properties. A decreasing Alane temperature is actually needed to maintain the pressure–volume energy in the dehydrogenation and storage chamber. This non-linear requirement can also be observed in Fig. 5(a) and (b) where a negative dT/dt and power are required to maintain the H_2 necessary for 30 W of continuous power from the fuel cell.

In Fig. 12(b), the heater requirements are recast in terms of the energy consumed by the heater over the 25 h period. Roughly 22 W h of energy consumed by the heater, which is rather modest compared to the 750 W h of the 30 W fuel cell system over this same period (500–625 W h usable). However, this energy loss can drastically increase if the system is cycled on and off, where at least the 22 W h of energy is compounded by the number of cycles.

Because the requirements of a hybrid battery are also of concern, Fig. 12(c) provides the power consumed from the battery. This includes both to power the heater during startup (i.e., prior to the H_2 storage chamber having 35 J of pressure–volume energy) and an additional 25 W to the user for an instant power startup. A constant load is assumed, so the battery is only required during startup and periods where the heater requires more than 5 W of power to sustain dehydrogenation. This result may not be typical for applications where load following is necessary and there may be a spike in the power demand. Fig. 12(d) recasts this in terms of the energy requirement from the battery to meet these startup demands, which is about 11.25 W h over a 15 min period. Interestingly, this is much less than that which was calculated in Fig. 6 of Section 3.7 (18.5 W h for a 15 min startup). In fact the axisymmetric model observes initial startup in approximately 15 min, with another 15 min worth of throttling where the H_2 pressure–volume energy rises above and falls below the 35 J minimum. The throttling behavior reduces the power being delivered by the heater over this period and thereby the energy requirement. Throttling aside, the discrepancy between the energy requirements for initially calculated and those predicted by the axisymmetric model are undoubtedly associated with the spatial variations in the dehydrogenation process during the initial heating of the Alane. This can be confirmed by noting that the isothermal model (not shown) calculates 20 W h of energy needed with a 24 min startup demonstrating; a much more consistent result. The spatial variations in the axisymmetric model leading to these discrepancies are shown in Fig. 13, which provides a contour plot of the temperature distributions in the Alane in the first 20 min of startup. During this initial transience, these variations are quite significant and account for discrepancies.

Within these results, it is recognized that it is possible to adequately control an Alane based H_2 storage material for operation in a high energy density, portable fuel cell system. However, it must be acknowledged that this study presented a narrow spectrum of

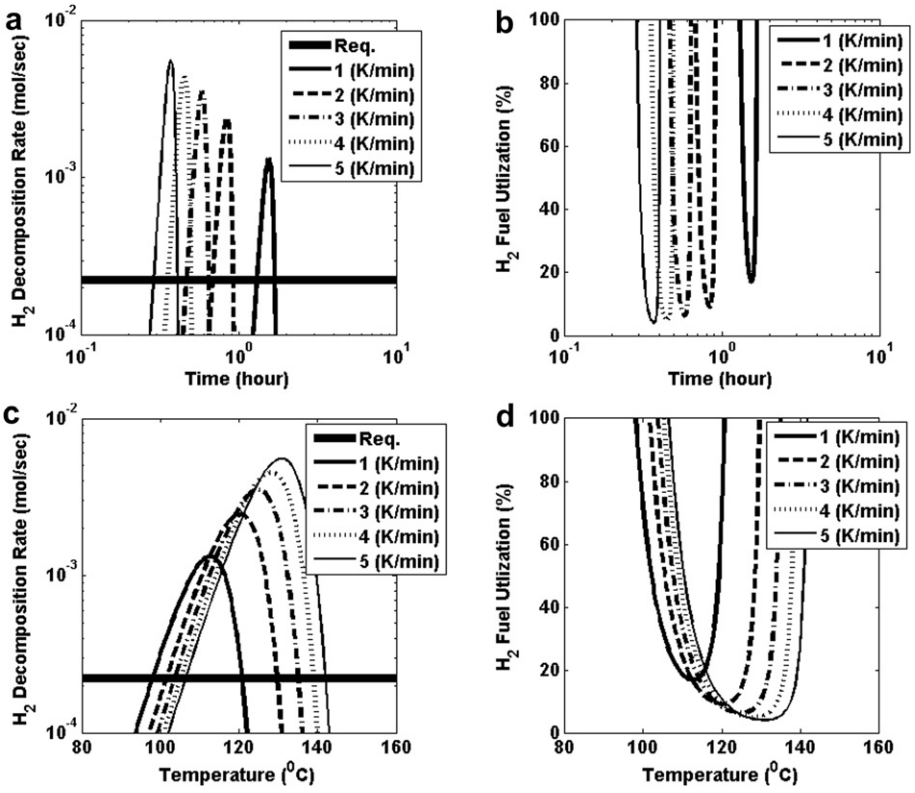

Fig. 10. Dehydrogenation of 0.2 kg of α-Alane is examined under constant heating as a function of the rate change in temperature, or heating rate. The (a) H_2 molar dehydrogenation rates and (b) percent H_2 fuel utilization are shown as a function of time. The (c) H_2 molar dehydrogenation rates and (d) percent H_2 fuel utilization are also shown as a function of temperature.

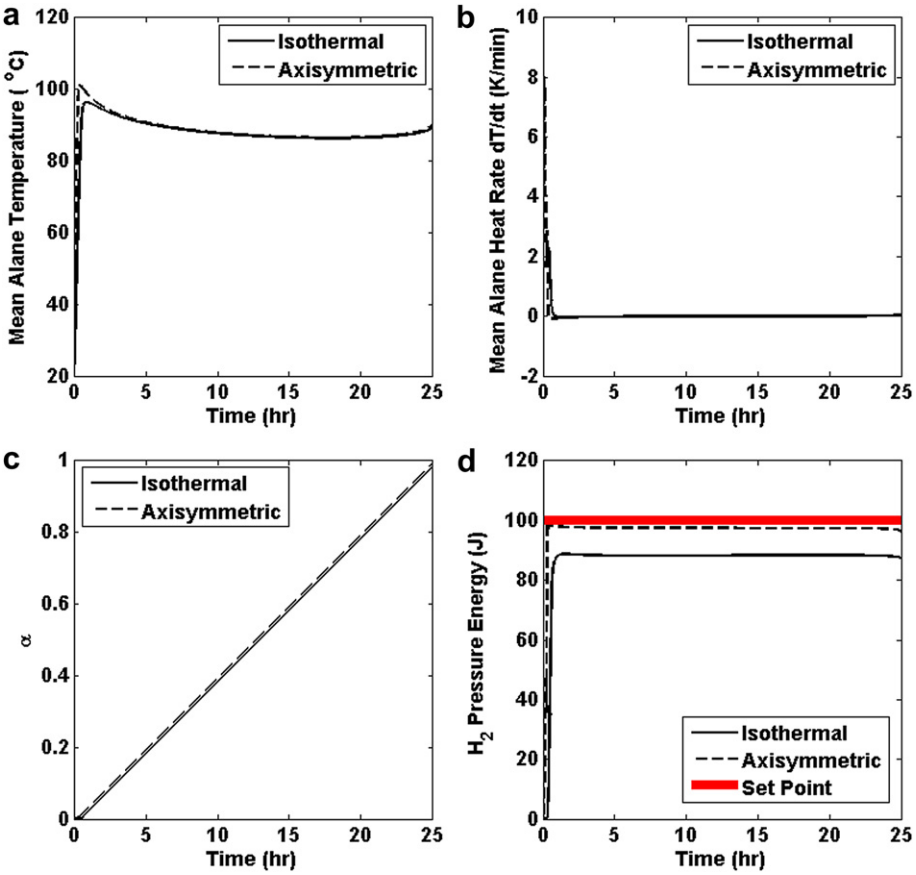

Fig. 11. A comparison of isothermal and axisymmetric Alane dehydrogenation models, including the volume weighted mean (a) Alane temperature, (b) heat rate, (c) extent of dehydrogenation, and the (d) H_2 pressure–volume energy accumulated in the dehydrogenation chamber and storage vessel.

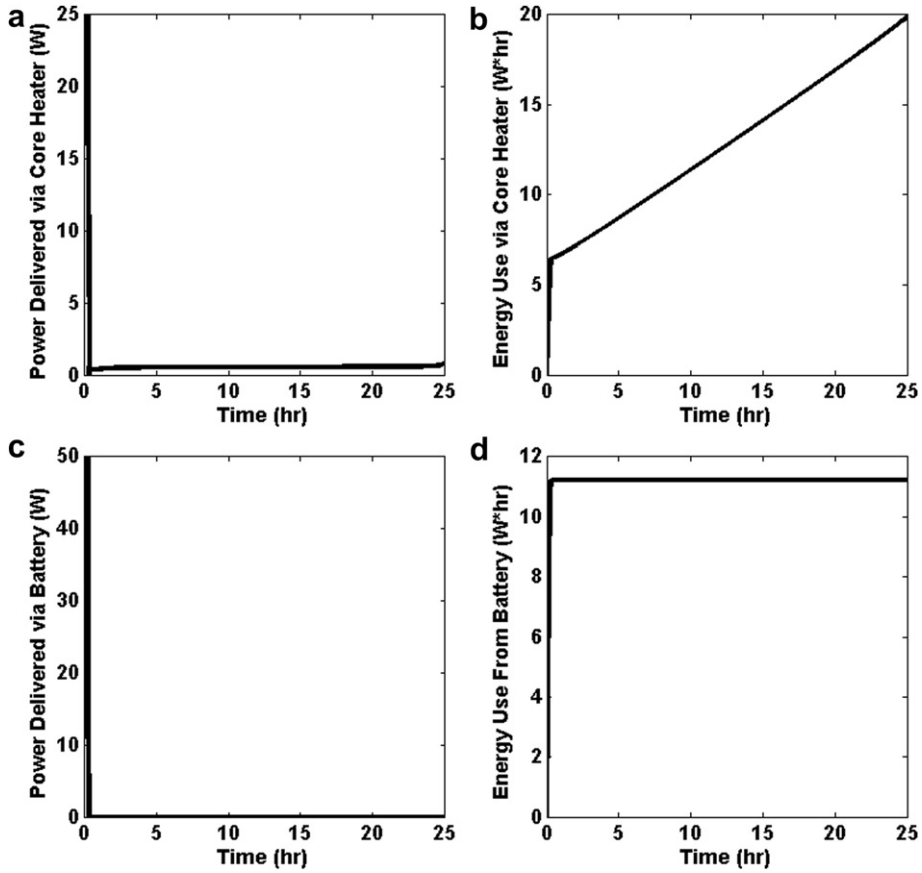

Fig. 12. In (a), the power requirement to startup the dehydrogenation process is provided, while (b) provides this in terms of the energy requirement for this process. In (c) 25 W of additional electrical power is provided from the hybrid battery for instant power and (d) the corresponding energy use from the hybrid battery. Results are from the axisymmetric model.

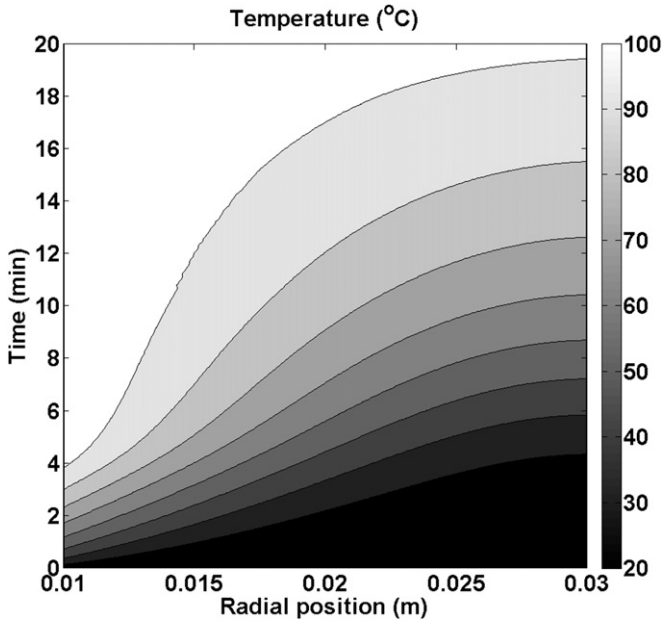

Fig. 13. Spatial variations in Alane temperature during the first 20 min of startup are provided. Radial variations in temperature are due to localized heating near the annulus core.

conditions. The much more rigorous challenge of designing around the unexpected and potential scenarios that the device may encounter in the field with appropriate failsafe mechanisms remains.

5. Conclusions

Alane has been examined as a possible solid fuel for use in a 30 W portable fuel cell system in this study, which is capable of providing 20–25 W of electrical power; the balance of plant consuming the remainder. The approximate volume and mass estimates of the Alane annulus (0.3 L, 0.4 kg), dehydrogenation chamber (0.6 L = 0.3 L H_2 Storage + 0.3 L Alane, est. 0.2 kg), hybrid battery (0.1 L, 0.245 kg), and a typical PEMFC with requisite balance of plant (est. 0.3 L, est. 0.2 kg) suggest this system is capable of running for approximately 25 h on 0.4 kg of Alane with a system volume and mass in the neighborhood of 1 L and 1 kg. This provides a gravimetric and volumetric specific energy (energy density) in the vicinity of 600 W h kg^{-1} and 600 W h L^{-1} over a continuous 25 h period. This would increase to approximately 1000 W h kg^{-1} and 1125 W h L^{-1} with an additional two 0.4 kg Alane fuel annuli to extend to a 72 h operation period. However, these values assume continuous operation. Undoubtedly, these values will drop significantly if the fuel cell power is cycled during this period, and/or there are requirements to purge H_2 from the onboard storage. There are opportunities to decrease both the volume and mass of the system by using smaller segments of Alane and thereby a smaller dehydrogenation and H_2 storage vessel. In principle, this can all be

completed in a single package offering a convenient form factor along with an exceptional energy density. However, it is stressed that this is a conceptual study and there are always discrepancies encountered when putting together an actual system. Further, not all scenarios of the practical use of such a system have been explored in this work.

This study demonstrates that benefits of using an Alane as a H_2 storage media for a portable fuel cell system are significant; however, so are the risks. A significant portion of this work was directed toward highlighting these risks. The most significant are those associated with an over-pressurization of the H_2 storage vessel. Such a failure could occur due to a disruption within the fuel cell system or a change in conditions. Also of concern with the use of Alane is that it is metastable in the vicinity of ambient and dehydrogenation conditions. If it is sufficiently perturbed, it could lead to a catastrophic event. For military applications there is prospect of projectiles, crushing, and extreme operational environments that raise concern.

Further, to the authors' knowledge, the synthesis of Alane is not presently being undertaken at mass industrial levels. At present, the synthesis methods tend to require extreme conditions and often expensive chemicals. Even with a significant scale up in the domestic production of Alane, there are logistical challenges. Alane must be stored at reasonable temperatures so that it doesn't dehydrogenate while in storage, along with the corresponding risks. The Alane fuel must reach the user in proper form. This means, that the Alane surface cannot undergo oxidation. Should the surface become oxidized, scales can form on the surface and thereby impeded the internal diffusion of H_2 during dehydrogenation. On the basis of these findings, we suggest that Alane does provide distinct advantages for use in high specific energy portable power sources. However, further materials and systems engineering are needed to adequately address significant issues related to its safe use.

Acknowledgments

Financial support from the U.S. Department of the Army and U.S. Army Materiel Command are gratefully acknowledged. Research was supported, in part, by an appointment to the U.S. Army Research Laboratory Postdoctoral Fellowship Program administered by the Oak Ridge Associated Universities through Cooperative Agreement Number W911NF-12-2-0019. The authors also gratefully acknowledge support of ZBB's contributions to this work, through the U.S. Military Academy's Advanced Individual Advanced Development program. Discussions with Dr. Tony Thampan, U.S. Army Communications-Electronics Research, Development and Engineering Center (CERDEC), are gratefully acknowledged.

References

[1] Assistant Secretary of Defense for Operational Energy Plans & Programs, Energy for the Warfighter: Operational Energy Strategy, U.S. Dept. of Defense, 2011.
[2] E. Bostic, N. Sifer, C. Bolton, U. Ritter, T. Dubois, J. Power Sources 137 (2004) 76–79.
[3] E.H. Yu, U. Krewer, K. Scott, Energies 3 (2010) 1499–1528.
[4] J.A. Kumar, P. Kalyani, R. Saravanan, Int. J. Electrochem. Soc. 3 (2008) 961–969.
[5] C. Lamy, E.M. Belgsir, J.M. Leger, J. Appl. Electrochem. 31 (2001) 799–809.
[6] A. Serov, C. Kwak, Appl. Catal. B Environ. 98 (2010) 1–9.
[7] B.K. Boggs, G.G. Botte, J. Power Sources 192 (2009) 573–581.
[8] K. Asazawa, T. Sakamoto, S. Yamaguchi, K. Yamada, H. Fujikawa, H. Tanaka, K. Oguro, J. Electrochem. Soc. 156 (2009) B509–B512.
[9] H.W. Li, Y.G. Yan, S. Orimo, A. Zuttel, C.M. Jensen, Energies 4 (2011) 185–214.
[10] H.W. Li, S. Orimo, Y. Nakamori, K. Miwa, N. Ohba, S. Towata, A. Zuttel, J. Alloy Comp. 446 (2007) 315–318.
[11] H. Senoh, Z. Siroma, N. Fujiwara, K. Yasuda, J. Power Sources 185 (2008) 1–5.
[12] J. Graetz, J.J. Reilly, V.A. Yartys, J.P. Maehlen, B.M. Bulychev, V.E. Antonov, B.P. Tarasov, I.E. Gabis, J. Alloy Comp. 509 (2011) S517–S528.
[13] J. Graetz, J.J. Reilly, J. Phys. Chem. B 109 (2005) 22181–22185.
[14] J. Graetz, S. Chaudhuri, J. Wegrzyn, Y. Celebi, J.R. Johnson, W. Zhou, J.J. Reilly, J. Phys. Chem. C 111 (2007) 19148–19152.
[15] B.M. Wong, D. Lacina, I.M.B. Nielsen, J. Graetz, M.D. Allendorf, J. Phys. Chem. C 115 (2011) 7778–7786.
[16] D. Lacina, J. Reilly, J. Johnson, J. Wegrzyn, J. Graetz, J. Alloy Comp. 509 (2011) S654–S657.
[17] D. Lacina, J. Reilly, Y. Celebi, J. Wegrzyn, J. Johnson, J. Graetz, J. Phys. Chem. C 115 (2011) 3789–3793.
[18] I.M. Robertson, D.D. Graham, J. Graetz, J. Reilly, J.E. Wegrzyn, J. Phys. Chem. C 114 (2010) 15207–15211.
[19] D. Lacina, J. Wegrzyn, J. Reilly, Y. Celebi, J. Graetz, Energ. Environ. Sci. 3 (2010) 1099–1105.
[20] D.D. Graham, J. Graetz, J. Reilly, J.E. Wegrzyn, I.M. Robertson, J. Phys. Chem. C 114 (2010) 15207–15211.
[21] J. Graetz, J. Wegrzyn, J.J. Reilly, J. Am. Chem. Soc. 130 (2008) 17790–17794.
[22] V.E. Antonov, A.I. Kolesnikov, Y.E. Markushkin, A.V. Palnichenko, Y. Ren, M.K. Sakharov, J. Phys. Condens. Mat. 20 (2008).
[23] C. Pohlmann, L. Röntzsch, J.L. Hu, T. Weißgärber, B. Kieback, M. Fichtner, J. Power Sources 205 (2012) 173–179.
[24] F.P. Incropera, D.P. DeWitt, Fundamentals of Heat and Mass Transfer, fifth ed., Wiley, New York, 2002.
[25] J. Graetz, J.J. Reilly, J.G. Kulleck, R.C. Bowman, J. Alloy Comp. 446 (2007) 271–275.
[26] J. Graetz, J.J. Reilly, J. Alloy Comp. 424 (2006) 262–265.